Transient Calculations of Two-Dimensional Eddy Current Problems

MIN EIG LEE, STUDENT MEMBER, IEEE, S. I. HARIHARAN, AND NATHAN IDA, SENIOR MEMBER, IEEE

Abstract—**In this paper we investigate a transient eddy current problem in two dimensions. The situation describes a transverse magnetic (TM) field incident on a good conductor. The resulting model is an interface problem with the continuities of tangential electric and magnetic fields being the interface conditions. An approximation of Sommerfeld's radiation condition is employed for the absorption of the high-frequency scattered wave. Finite difference methods are used for discretization. Instabilities arising from implementing the radiation condition and implementation of the interface conditions make the problem harder for numerical treatment. In addition, low-frequency situations require special treatment of radiation conditions. We present our procedures to overcome the difficulties and validate our numerical results with the analytic solutions.**

Introduction

EDDY CURRENTS are induced in a conductor when an electromagnetic field is incident upon it. Calculation of eddy currents is therefore an interface problem with the boundary of the conductor being the interface. A common way of treating these problems is to estimate an appropriate skin depth for the conductor and obtain the associated fields through an equivalence principle [1]. The skin depth is obtained by the field penetration into an infinite planar slab. However, if the conductor happens to have a different geometry, the procedure will not work well. In general, the incident fields need not be time-harmonic. Pulse sources and surge waves from thunder or circuit breakers occur in common practice. Therefore, one must have a procedure to capture the transient behavior of eddy currents. Along this line, Hariharan and MacCamy [2] solved the problem in the frequency domain using integral equation procedures. Our goal is to model the eddy current problems in an unbounded region and to solve these problems, in particular, a two-dimensional problem in the time domain, using finite difference methods.

Formulation of the Problem

Consider a conduting cylinder parallel to the z axis. The incident field has the form: $\boldsymbol{E}_i = E_i(x, y, t)\boldsymbol{k}$ and $\boldsymbol{H}_i = H_{i1}(x, y, t)\boldsymbol{i} + H_{i2}(x, y, t)\boldsymbol{j}$. Maxwell's equations for this situation are

$$\frac{\partial H_1}{\partial x} + \frac{\partial H_2}{\partial y} = 0 \tag{1}$$

$$\frac{\partial E}{\partial y}\boldsymbol{i} - \frac{\partial E}{\partial x}\boldsymbol{j} = -\mu\left(\frac{\partial H_1}{\partial t}\boldsymbol{i} + \frac{\partial H_2}{\partial t}\boldsymbol{j}\right) \tag{2}$$

$$\frac{\partial H_2}{\partial x} - \frac{\partial H_1}{\partial y} = \sigma E + \epsilon\frac{\partial E}{\partial t} \tag{3}$$

where μ, ϵ, and σ are material properties in both regions and assumed to be frequency-independent and isotropic. We assume that $\sigma = 0$ in air. In addition, the tangential components of $\boldsymbol{E}$ and $\boldsymbol{H}$ are continuous on the interface and the scattered $\boldsymbol{E}$ and $\boldsymbol{H}$ both decay to zero at infinity. Equation (1) suggests the existence of a scalar function Ψ such that $H_1 = \partial\Psi/\partial y$ and $H_2 = -\partial\Psi/\partial x$. Using this function in the nondimensional form [3], one can obtain the following scalar problem which is solved in a truncated region:

$$\frac{\partial^2\Psi}{\partial x^2} + \frac{\partial^2\Psi}{\partial y^2} = \frac{\partial^2\Psi}{\partial t^2}, \qquad \text{in air} \tag{4}$$

$$\frac{\partial^2\Psi}{\partial x^2} + \frac{\partial^2\Psi}{\partial y^2} = l_m^2\frac{\partial\Psi}{\partial t} + k_m^2\frac{\partial^2\Psi}{\partial t^2}, \qquad \text{in conductor} \tag{5}$$

where

$$l_m^2 = \frac{\omega L^2\mu_m\sigma_m}{\omega L\sqrt{\mu_a\epsilon_a}} \qquad k_m^2 = \frac{\omega^2L^2\mu_m\epsilon_m}{\omega^2L^2\mu_a\epsilon_a}$$

L is a length for scaling and is on the order of the conductor's diameter. On the interface, $\mu_a\Psi^- = \mu_m\Psi^+$ and $\partial\Psi^-/\partial n = \partial\Psi^+/\partial n$, where the minus sign indicates the exterior field and the plus sign the interior field. Initial conditions are $\Psi(x, y, 0) = \Psi_i(x, y, 0)$ and $\partial\Psi/\partial t(x, y, 0) = \partial\Psi_i/\partial t(x, y, 0)$. The radiation condition is

$$\frac{\partial\Psi_s}{\partial r} + \frac{\partial\Psi_s}{\partial t} + A(r)\Psi_s = 0$$

where

$$A(r) = \frac{1}{2r}, \qquad \text{far field} \tag{6}$$

Manuscript received February 7, 1989. This paper was presented at the 4th Joint MMM-INTERMAG Conference, Vancouver, BC, Canada, July 12-15, 1988.

The authors are with the Department of Electrical Engineering, University of Akron, Akron, OH 44325.

IEEE Log Number 8927728.

0018-9464/89/0700-3140$01.00

$$= \frac{1}{r}\left[-\frac{1}{\gamma - \ln 2 + \ln k_a + \ln r}\right], \qquad \text{near field} \tag{7}$$

where Ψ_s is the scattered field, $k_a = \omega L\sqrt{\mu_a \epsilon_a}$, and γ is Euler's constant. Equation (6) is an approximation to Sommerfeld's radiation condition [4]. The distance of a far-field boundary requires at least one wavelength. It is not practical for the low-frequency electromagnetic waves. Therefore, we developed (7) to deal with this case. Derivation of this condition can be found in [3].

Numerical Method

The problem is solved by an explicit finite difference method. On the radiation boundary, the total field consists of two components: the incident field Ψ_i and the scattered field Ψ_s. The radiation condition takes care of the scattered field only. The origin is located at the center of the scatterer. In Cartesian coordinates, (6) has the form

$$\frac{\partial \Psi_s}{\partial x}\cos\theta + \frac{\partial \Psi_s}{\partial y}\sin\theta + \frac{\partial \Psi_s}{\partial t} + \frac{\Psi_s}{2r} = 0. \tag{8}$$

Finite difference methods have difficulties at the corners of a rectangular radiation boundary. These are due to conflicts of the difference formulas at the corners. As a result, these corners become sources of instability. In this work, a method using a smooth transition was developed to solve corner problems. The approach is depicted in Fig. 1. On the boundary A_1 to A_2, $\partial\Psi_s/\partial x$ is implemented by a forward-difference formula and $\partial\Psi_s/\partial y$ by a backward-difference formula. On the boundary B_1 to B_2, both are implemented by backward-difference methods. It seems that implementation of $\partial\Psi_s/\partial x$ will conflict at the intersection point C. But, since the term is multiplied by $\cos\theta$ and its value is 0 at C, the conflict cannot take effect and corner problems are avoided.

The interface boundary is approximated by a polygon whose vertices occupy the regular grids. For example, the circle Γ in Fig. 2(a) is approximated by the polygon Γ'. The field computation is then classified into two categories: exterior and interior. For points on the boundary, if the grid separation is much larger than the skin depth, the interior equation is used. Otherwise, the exterior equation is used. The second interface condition can be changed to

$$\frac{\partial \Psi^-}{\partial x}\cos\theta + \frac{\partial \Psi^-}{\partial y}\sin\theta = \frac{\partial \Psi^-}{\partial x}\cos\theta + \frac{\partial \Psi^+}{\partial y}\sin\theta \tag{9}$$

where θ is the angle between the normal direction and the x axis. Since $\cos\theta$ and $\sin\theta$ are linearly independent, we have: $\partial\Psi^-/\partial x = \partial\Psi^+/\partial x$ and $\partial\Psi^+/\partial y = \partial\Psi^+/\partial y$ on the interface boundary. With these, when the field computation involves a point in the other region, an equivalent value at that point can be obtained for calculation. For example, the equivalent value of Ψ^- at B in Fig. 2(b) can be obtained from

$$\Psi_B^- = \Psi_B^+ + (1 - 1/\mu_r)\Psi_A^-. \tag{10}$$

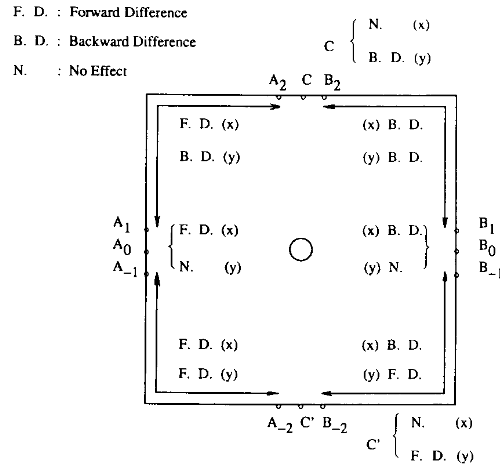

Fig. 1. Implementation of the radiation condition.

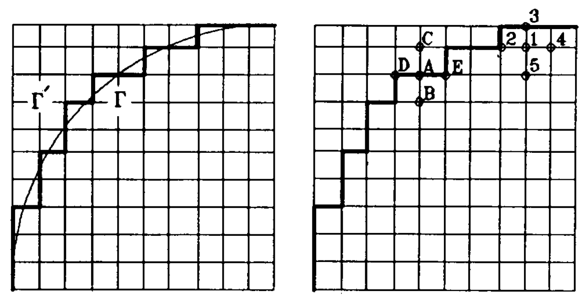

(a) (b)

Fig. 2. (a) Approximating a curve with a polygon. (b) Grid points near the interface boundary.

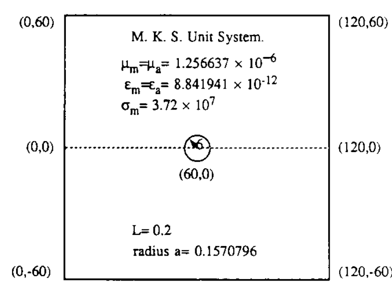

Fig. 3. Mesh size and parameters for the first two situations.

Numerical Experiments

Using the previous method, we consider three situations described herein. The incident fields are assumed to be plane waves and incident on the left boundary starting from $t = 0$. For the first two cases, the conductor is a circular cylinder of aluminum. The grid coordinates and the parameters used are shown in Fig. 3.

In the first situation, the incident field is $\Psi_i = \cos(k_a(x - t))$. A high frequency of 2.387324×10^8 Hz is used. $k_a = 1$, $l_m^2 = 2.804814 \times 10^9$, and $k_m^2 = 1$. The numerical solution in a steady state is shown in Fig. 4. Aluminum behaves close to a perfect conductor in the high-frequency

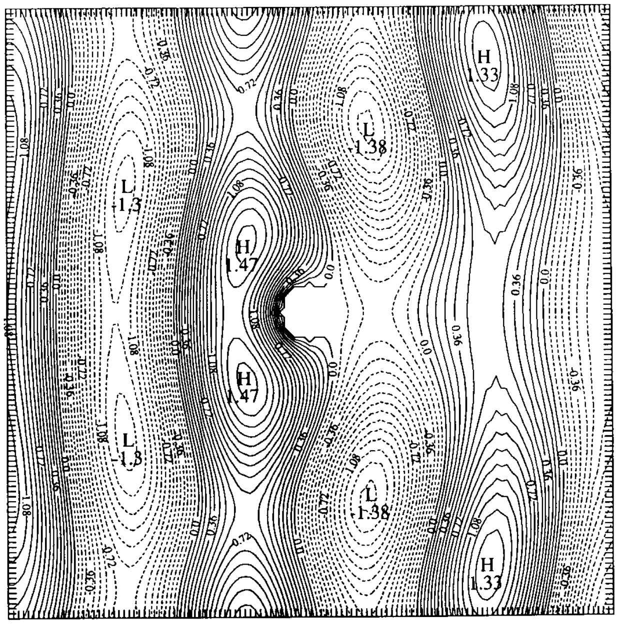

Fig. 4. Contour plot of the numerical solution, $f = 2.387324 \times 10^8$ Hz, result obtained after 10 periods.

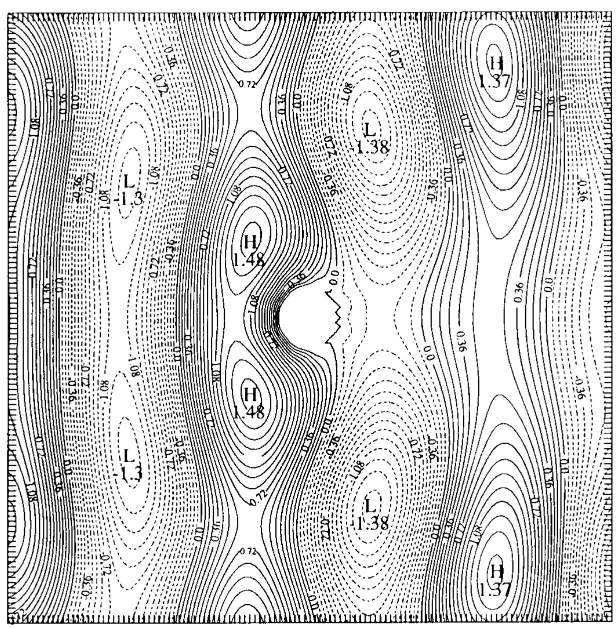

Fig. 5. Approximate analytic solution of Fig. 4.

case. The analytic solution for the perfect-conductor problem was found in [5] and plotted in Fig. 5. Comparing Figs. 4 and 5, we find that both solutions are in a good agreement. The numerical solution demonstrates a tendency of field penetration into the conductor. Deeper penetration occurs on the illuminated side. The difference near the artificial boundary comes from the fact that its distance from the center is not infinite. This tradeoff, however, makes the numerical implementation on a computer possible and efficient.

In the second situation, the incident field has a Gaussian time variation. After scaling, it has the form

$$\Psi_i = \exp\left(-k_g^2(x - t + t_0)^2\right). \tag{11}$$

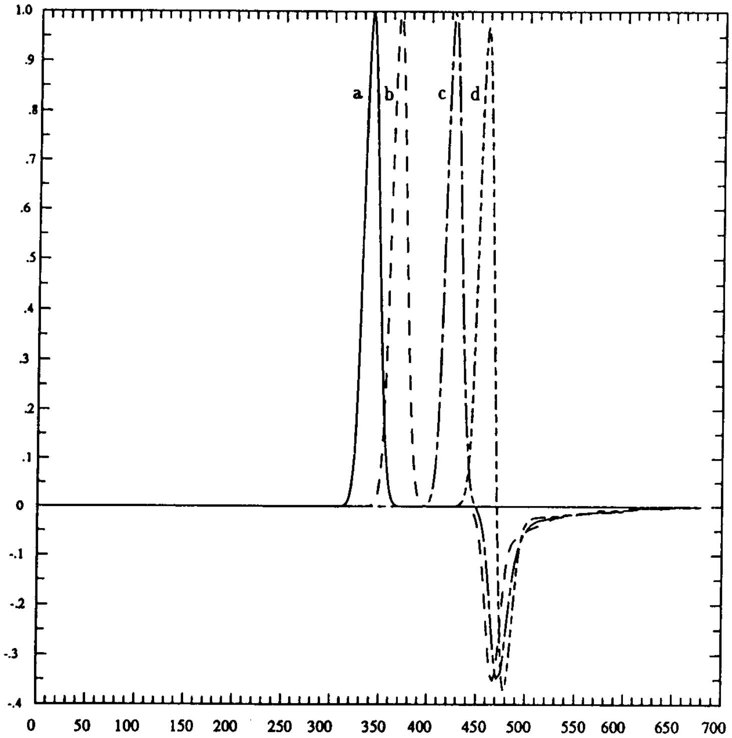

Fig. 6. *a*—Short-pulse source. *b*—History plot at $P_1(20, 0)$. *c*—History plot at $P_2(60, 40)$. *d*—History plot at $P_3(84, 32)$.

When $k_g = 1$, it becomes a short pulse as shown in Fig. 6 as *a*. Using (6), we obtain the history plots at $P_1(20, 0)$, $P_2(60, 40)$, and $P_3(84, 32)$ in Fig. 6 as *b*, *c*, and *d*, respectively. These plots display distinctly the incident waves and the scattered waves. The scattered waves decay with increasing distance from the scattering center. Since three points are at the same distance from the scattering center, the amplitudes of three scattered waves are found almost the same. The time interval between the peak and the valley represents the time delay of the scattered wave. Comparisons of these delays to those obtained from geometrical optics are listed in Table I. From this point of view, the numerical result is found to be satisfactory.

Using our method, some results in the low-frequency single-conductor case are validated with the analytic solutions in [3]. As an extension of that work, we consider a low-frequency two-conductor situation here. The conductors are circular cylinders of graphite. $\mu_m = \mu_a$, $\epsilon_m = \epsilon_a$, $\sigma_m = 4 \times 10^4$ S/m, $L = 0.05$ m, and $a = 0.6544985 \times 10^{-1}$ m. The mesh size used is 49 points × 25 points. The incident field is sinusoidal with a frequency of 6000 Hz. $k_a = 6.283185 \times 10^{-6}$, $l_m^2 = 7.539822 \times 10^5$, and $k_m^2 = 1$. A grid separation of 0.6544985×10^{-2} m, which is about 1/5 skin depth, is chosen. The near-field condition is imposed on the artificial boundary. The numerical result after one period is shown in Fig. 7. In this case, no analytic solution is available for comparison. A similar contour for the power flow density of a two-conductor transmission line was found in [6, p. 471]. Only the outside field was considered there. However, Fig. 7 displays a clear view of the field distribution near and inside the interface boundary.

TABLE I
TIME DELAY OF SCATTERED WAVES
(1 unit = 6.170671×10^{-11} s)

Point	Numerical Result	Geometrical Optics
(20, 0)	98	96
(60, 40)	48	45
(84, 32)	20	16

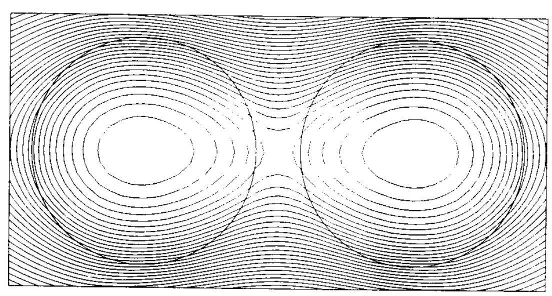

Fig. 7. Contour plot of the two-conductor case, f = 6000 Hz, result obtained after 1 period.

Conclusion

The two-dimensional eddy current problem has been modeled in the time domain and successfully solved by explicit finite difference methods. The numerical results justified by the analytic solutions show that the model is practical and the numerical treatment is correct. In high-frequency cases, the far-field condition (6) can be used to solve practical problems. In low-frequency cases, the near-field condition (7) is more powerful. It reduces the mesh size and makes the calculations near and inside the boundary feasible. Furthermore, the method can deal with nonsinusoidal fields. In this paper, a short pulse has been successfully used as the incident field.

References

[1] J. A. Kong, *Electromagnetic Wave Theory*. New York, NY: Wiley, 1986, pp. 358-367.

[2] S. I. Hariharan and R. C. MacCamy, "Integral equation procedures for eddy current problems," *J. Comput. Phys.*, vol. 45, no. 1, pp. 81-99, 1982.

[3] M. E. Lee, S. I. Hariharan, and N. Ida, "Solving time-dependent two-dimensional eddy current problems," NASA ICOMP Rep., Lewis Research Center, pp. 88-100, June 1988.

[4] S. I. Hariharan and T. H. Moulden, *Numerical Methods for Partial Differential Equations*. London, UK: Longmans, 1986, pp. 199-232.

[5] J. Van Bladel, *Electromagnetic Fields*. Washington, DC: Hemisphere Publ., 1985, pp. 376-382.

[6] J. D. Krause, *Electromagnetics*. New York, NY: McGraw-Hill, 1984, pp. 471.

Min Eig Lee (S'88) was born in Yenshui, Taiwan, ROC, in 1952. He received the B.S. and M.S. degrees in electrical engineering, from the National Taiwan University, Taipei, Taiwan, ROC in 1974, and Youngstown State University, Youngstown, OH, in 1986, respectively. He received the Ph.D. degree from the University of Akron, Akron, OH, in May 1989.

From 1976 to 1985, he worked at a technological school, where he lectured and conducted experiments in power engineering. His recent research is concentrated on computation of electromagnetic fields, especially for time-dependent interface problems.

Dr. Lee is a member of the IEEE Societies of Magnetics, Antennas and Propagation, and Microwave Theory and Techniques.

S. I. Hariharan was born in Jaffna, Sri Lanka, on October 27, 1951. He received the B.Sc. degree from the University of Sri Lanka in 1974, the M.Sc. degree from the University of Salford, Salford, England, in 1978, and the M.S. and Ph.D. degrees from Carnegie-Mellon University, Pittsburgh, PA, in 1979 and 1980, respectively.

He has been with ICASE at NASA, Langley Research Center as a staff scientist, at the University of Tennessee Space Institute as an assistant professor, and at the University of Akron, where he is an Associate Professor of Mathematics. His primary interests are in applied mathematics, acoustics, and electromagnetic wave propagation and fluid mechanics.

Dr. Hariharan is a member of SIAM and AMS.

Nathan Ida (S'82-M'83-SM'87) was born in Roumania on December 12, 1949. He received the B.Sc. and M.Sc. degrees in electrical engineering from Ben-Gurion University, Beer Sheva, Israel, in 1977 and 1979, respectively, and the Ph.D. degree in electrical engineering from Colorado State University, Fort Collins, in 1983.

He is currently Associate Professor of Electrical Engineering at the University of Akron, Akron, OH, where he is teaching electromagnetic fields and numerical methods. His industrial research experience includes consulting work with Teledyne Water Pik, NUMAR, TECHNICARE, and ARCOVA Corporations. His current research interests are in the area of numerical modeling of electromagnetic fields, electromagnetic wave propagation, nondestructive testing, and parallel and vector computation.

Dr. Ida is a senior member of the IEEE Magnetics and Computer Societies and member of the American Society for Nondestructive Testing.